

Posterior Ratio Estimation for Latent Variables

Yulong Zhang, Mingxuan Yi, Song Liu *
Mladen Kolar[†]

Abstract

Density Ratio Estimation has attracted attention from machine learning community due to its ability of comparing the underlying distributions of two datasets. However, in some applications, we want to compare distributions of *latent* random variables that can be only inferred from observations. In this paper, we study the problem of estimating the ratio between two posterior probability density functions of a latent variable. Particularly, we assume the posterior ratio function can be well-approximated by a parametric model, which is then estimated using observed datasets and synthetic prior samples. We prove consistency of our estimator and the asymptotic normality of the estimated parameters as the number of prior samples tending to infinity. Finally, we validate our theories using numerical experiments and demonstrate the usefulness of the proposed method through some real-world applications.

1 Introduction

Comparing the underlying distributions of two given datasets has been an important task in machine learning community and has a wide range of applications. For example, change detection algorithms Kawahara and Sugiyama ((2012)) compare datasets collected at different time points and report how the underlying distribution has shifted over time; Transfer learning algorithms Quionero-Candela et al. ((2009)) utilize the estimated differences between two datasets to efficiently share information between different tasks. Generative Adversarial Net (GAN) Goodfellow et al. ((2014)) learns an implicit generative model whose output minimizes the differences between an artificial dataset and a real dataset.

Various computational methods have been proposed for comparing underlying distributions given two sets of observations. For example, Maximum Mean Discrepancy (MMD) Gretton et al. ((2012)) computes the distance between the kernel mean embeddings of two datasets in Reproducing Kernel Hilbert Space (RKHS). Density ratio estimation (DRE) Sugiyama et al. ((2012a)) estimates the ratio function between two probability densities. The estimated ratio has natural links with various statistical divergences Sugiyama et al. ((2012b)); Nowozin et al. ((2016)). Recently, Wasserstein distance (and Optimal Transport distance) as an alternative to statistical divergence has been explored for many learning tasks Frogner et al. ((2015)); Arjovsky et al. ((2017)) and efficient algorithms for computing such a distance from two sets of samples have been proposed Genevay et al. ((2016)).

However in some applications we are not interested in comparing distributions of observed random variables. Instead we hope to compare distributions of *unobserved* random variables given observed datasets. For example, in civil engineering, we can collect accelerometer readings in a building at two different time points. We would like to know how the structural stiffness has changed over time. Here, the structural stiffness is a latent variable whose *posterior* distribution have to be inferred from observed readings, a likelihood function and a prior. To make things more challenging, the exact computation of the likelihood function is sophisticated and is expensive to evaluate, thus given a limited computational budget, we are only allowed to evaluate the likelihood function within a limited number of times.

One straightforward approach of comparing posteriors is representing two posterior probabilities in the form of two *different* likelihood functions and two *different* priors using Bayes rule and evaluating them

*University of Bristol, UK

[†]University of Chicago, Booth School of Business, US

at some ‘‘anchor points’’. We can see how much the computed values differ at those points and deduce how much two posteriors differ. However, it is not very obvious how to select such anchor points in a high dimensional space. One strategy is to select anchor points from samples of priors (note priors may differ). Then, it is unclear how to compare two posteriors when they are evaluated at different anchor points.

Approximate Bayesian Inference can be an alternative solution. We can select a simple parametric distribution for approximating the posterior, e.g. multivariate normal, then fit parameters of such a distribution by minimizing KL divergence of the distribution from the real posterior. This procedure is usually referred as Variational Inference (VI) Blei et al. ((2017)). Applying VI twice on two observed datasets yields two fitted models. Then we can compare them and work out the differences between two posteriors. However, the drawback of VI, which comes from the approximation of posteriors, can be worsened when performing VI *twice* for posterior comparison. Since computing the differences between two distributions is our target, we should only make model assumption *once* on the difference, rather than on individual posteriors.

Following this rationale, we develop a novel algorithm which compares two posterior probabilities by approximating their ratio directly. The algorithm is referred as Posterior Ratio Estimation (PRE) and can be regarded as an analogue of DRE for posterior probabilities. We assume two likelihood functions and two sets of prior samples are given. Likelihood functions can only be evaluated at some given sample points from priors. Our algorithm approximates the true posterior ratio by minimizing the KL divergence of one posterior from the other posterior reweighed by our ratio model. We prove that the estimated model parameter eventually converges to the true minimizer of the KL divergence, as the number of the prior samples increases. The estimated parameters are asymptotically normal which is useful for statistical inference. We evaluate the performance of our proposed algorithm on two applications: Neural net model comparison and Approximate Maximum *a Posteriori*. Promising results are obtained.

2 Posterior Ratio Estimation

2.1 Problem Setting

Suppose we have two observed datasets: X_p, X_q , two likelihood functions: $p(X_p|\mathbf{z})$, $q(X_q|\mathbf{z})$, and synthetic samples

$$Z_p := \{\mathbf{z}_p^{(i)}\}_{i=1}^{n_p}, Z_q := \{\mathbf{z}_q^{(i)}\}_{i=1}^{n_q},$$

drawn from two prior probabilities: $p(\mathbf{z})$, $q(\mathbf{z})$ where $\mathbf{z} \in \mathbb{R}^d$ is the *latent variable*.

Our target: approximate $\frac{p(\mathbf{z}|X_p)}{q(\mathbf{z}|X_q)}$ up to a constant.

- We do not require any explicit expression of $p(\mathbf{z})$ or $q(\mathbf{z})$. Only synthetic samples from the priors are needed. This can be advantageous as we are allowed to use samples from priors without explicit expressions.
- As previously mentioned, it is important to set a budget limit for evaluating the likelihood functions. In our setting, we assume evaluating $p(X_p|\mathbf{z}_p)$ and $q(X_q|\mathbf{z}_q)$ for all $\mathbf{z}_p, \mathbf{z}_q$ *exactly once* is within our computational budget.
- Note that if the likelihood functions can be easily evaluated and the explicit forms of the priors are known, one can directly compute $\frac{p(X_p|\mathbf{z})p(\mathbf{z})}{q(X_q|\mathbf{z})q(\mathbf{z})}$ which is the posterior ratio up to a constant. Apparently, this is not the setting considered by this paper.

2.2 Posterior Ratio Model

We model the posterior ratio using a parametric function,

$$r(\mathbf{z}; \boldsymbol{\delta}) := \frac{\exp\langle \boldsymbol{\delta}, \mathbf{f}(\mathbf{z}) \rangle}{Z(\boldsymbol{\delta})}, \tag{1}$$

where

$$\begin{aligned} Z(\boldsymbol{\delta}) &:= \int q(\mathbf{z}|X_q) \exp\langle \boldsymbol{\delta}, \mathbf{f}(\mathbf{z}) \rangle d\mathbf{z} \\ &= \int \frac{q(X_q|\mathbf{z})}{q(X_q)} \cdot q(\mathbf{z}) \exp\langle \boldsymbol{\delta}, \mathbf{f}(\mathbf{z}) \rangle d\mathbf{z}, \end{aligned}$$

and \mathbf{f} is a feature function chosen beforehand. In our experiments, we use polynomial features, $\mathbf{f}(\mathbf{z}) = [\mathbf{z}, \mathbf{z}^2]^\top$, which yields good results¹. $Z(\boldsymbol{\delta})$ ensures that the ratio model is properly normalized: for any $\boldsymbol{\delta}$,

$$\int q(\mathbf{z}|X_q) r(\mathbf{z}; \boldsymbol{\delta}) d\mathbf{z} = 1.$$

This model assumption implies that the true posterior ratio should be well-approximated by a log-linear model. Note that if both $p(\mathbf{z}|X_p)$ and $q(\mathbf{z}|X_q)$ are from the same exponential family, then the density ratio model is well-specified.

The feature function \mathbf{f} can be a highly complicated function and we do *not* assume $Z(\boldsymbol{\delta})$ has a closed form expression as it will be approximated using empirical samples from $q(\mathbf{z})$.

2.3 Posterior Ratio Estimation

We estimate $\boldsymbol{\delta}$ in the ratio model $r(\mathbf{x}; \boldsymbol{\delta})$ by minimizing the KL divergence from $p(\mathbf{z}|X_p)$ to $r(\mathbf{z}; \boldsymbol{\delta})q(\mathbf{z}|X_q)$:

$$\begin{aligned} \text{KL}[p|r \cdot q] &:= \int p(\mathbf{z}|X_p) \log \frac{p(\mathbf{z}|X_p)}{q(\mathbf{z}|X_q)r(\mathbf{z}; \boldsymbol{\delta})} d\mathbf{z} \\ &= C - \int p(\mathbf{z}|X_p) \log r(\mathbf{z}; \boldsymbol{\delta}) d\mathbf{z} \\ &= C - \frac{1}{p(X_p)} \int p(X_p|\mathbf{z})p(\mathbf{z}) \log r(\mathbf{z}; \boldsymbol{\delta}) d\mathbf{z}, \end{aligned}$$

where C and $p(X_p)$ do not depend on $\boldsymbol{\delta}$. Therefore, the minimization problem becomes:

$$\min_{\boldsymbol{\delta}} - \int p(X_p|\mathbf{z})p(\mathbf{z}) \log r(\mathbf{z}; \boldsymbol{\delta}) d\mathbf{z}. \quad (2)$$

Our approach is related to a DRE algorithm called Kullback-Leibler Importance Estimation Procedure (KLIEP) Sugiyama et al. ((2008)); Tsuboi et al. ((2009)). Details will be discussed in the related work section.

Let $l_p(\mathbf{z}), l_q(\mathbf{z})$ denote the likelihood functions $p(X_p|\mathbf{z}), q(X_q|\mathbf{z})$ and $\int p(\mathbf{z})\mathbf{f}(\mathbf{z})d\mathbf{z} =: \mathbb{E}_{p_{\mathbf{z}}}[f(\mathbf{z})]$. After replacing $r(\mathbf{z}; \boldsymbol{\delta})$ with its definition, the minimization problem in (2) can be written as

$$\min_{\boldsymbol{\delta}} \mathbb{E}_{p_{\mathbf{z}}} [l_p(\mathbf{z}) \cdot \langle -\boldsymbol{\delta}, \mathbf{f}(\mathbf{z}) \rangle] + \mathbb{E}_{p_{\mathbf{z}}} [l_p(\mathbf{z})] \cdot \log \mathbb{E}_{q_{\mathbf{z}}} \left[\frac{l_q(\mathbf{z})}{q(X_q)} \cdot \exp\langle \boldsymbol{\delta}, \mathbf{f}(\mathbf{z}) \rangle \right]. \quad (3)$$

Proposition 1. *A $\boldsymbol{\delta}^*$ is the minimizer of (2) if and only if*

$$\mathbb{E}_{p_{\mathbf{z}}} [l_p(\mathbf{z})\mathbf{f}(\mathbf{z})] = p(X_p) \cdot \mathbb{E}_{q_{\mathbf{z}}} \left[\frac{l_q(\mathbf{z})}{q(X_q)} \cdot r(\mathbf{z}; \boldsymbol{\delta}^*)\mathbf{f}(\mathbf{z}) \right]. \quad (4)$$

Proof. This statement can be easily verified by taking the derivative of the objective function in (3) and setting it to zero. Then applying the equality $\mathbb{E}_{p_{\mathbf{z}}}[l_p(\mathbf{z})] = p(X_p)$ yields the desired result. \square

If $p(X_p) > 0$, (4) can be rewritten as

$$\mathbb{E}_{p(\mathbf{z}|X_p)} [\mathbf{f}(\mathbf{z})] = \mathbb{E}_{q(\mathbf{z}|X_q)} [r(\mathbf{z}; \boldsymbol{\delta}^*)\mathbf{f}(\mathbf{z})].$$

This relationship implies that the expectation of $\mathbf{f}(\mathbf{z})$ with respect to the posterior $p(\mathbf{z}|X_p)$ equals to the expectation with respect to $q(\mathbf{z}|X_q)$ using $r(\mathbf{z}; \boldsymbol{\delta}^*)$ as the importance weighting function.

¹Here the power is applied elementwise.

2.4 Estimation Using Samples From Priors

Using two prior sample sets Z_p and Z_q , we can replace the expectations in (3) with empirical averages:

$$\hat{\boldsymbol{\delta}} := \underset{\boldsymbol{\delta}}{\operatorname{argmin}} -\hat{\mathbb{E}}_{p_{\mathbf{z}}} [l_p(\mathbf{z}) \cdot \langle \boldsymbol{\delta}, \mathbf{f}(\mathbf{z}) \rangle] + \hat{p}(X_p) \cdot \log \hat{\mathbb{E}}_{q_{\mathbf{z}}} [l_q(\mathbf{z}) \cdot \exp \langle \boldsymbol{\delta}, \mathbf{f}(\mathbf{z}) \rangle] + C', \quad (5)$$

where

$$\begin{aligned} \hat{\mathbb{E}}_{p_{\mathbf{z}}} [f(\mathbf{z})] &:= \frac{1}{n_p} \sum_{i=1}^{n_p} f(\mathbf{z}_p^{(i)}), & \hat{p}(X_p) &:= \hat{\mathbb{E}}_{p_{\mathbf{z}}} [l_p(\mathbf{z})], \\ \hat{\mathbb{E}}_{q_{\mathbf{z}}} [f(\mathbf{z})] &:= \frac{1}{n_q} \sum_{i=1}^{n_q} f(\mathbf{z}_q^{(i)}), & \hat{q}(X_q) &:= \hat{\mathbb{E}}_{q_{\mathbf{z}}} [l_q(\mathbf{z})], \end{aligned}$$

and $C' = -\hat{p}(X_p) \log \hat{q}(X_q)$, which does not need to be evaluated when estimating $\hat{\boldsymbol{\delta}}$. For simplicity, we denote the objective function in (5) as $\ell(\boldsymbol{\delta})$.

The objective of (5) is convex with respect to $\boldsymbol{\delta}$ and the gradient descent can be used to find $\hat{\boldsymbol{\delta}}$. By precomputing $l_p(\mathbf{z}_p^{(i)})$ and $l_q(\mathbf{z}_q^{(i)})$ before the optimization, minimizing (5) will not exceed our likelihood function computational budget.

3 Consistency Analysis of $\hat{\boldsymbol{\delta}}$

In this section, we prove $\hat{\boldsymbol{\delta}}$ is consistent under mild regularity conditions. For simplicity, we assume our likelihood functions are bounded: there exists $L > 0$,

$$\infty > L \geq l_p(\mathbf{z}_p^{(i)}), l_q(\mathbf{z}_q^{(j)}) \geq \frac{1}{L} > 0, \forall i, j.$$

Notations. $\|\mathbf{a}\|$ is the ℓ_2 norm of a vector \mathbf{a} . $\|\mathbf{A}\|$ is the spectral norm of a matrix \mathbf{A} . $S(\mathbf{a}, R)$ is a sphere centered at \mathbf{a} with radius R . $\nabla_{\mathbf{a}} f(\mathbf{a}_0)$ is the gradient of $f(\mathbf{a})$ evaluated at \mathbf{a}_0 . $\lambda_{\min}(\mathbf{A})$ is the minimum eigenvalue of a matrix \mathbf{A} . “w.h.p” stands for with high probability. $\xrightarrow{\mathbb{P}}$ and \rightsquigarrow denote convergence in probability and in distribution, respectively.

3.1 Consistency of $\hat{\boldsymbol{\delta}}$ and Its Sufficient Conditions

We first state a main theorem with a list of sufficient conditions under which our estimator $\hat{\boldsymbol{\delta}}$ converges to $\boldsymbol{\delta}^*$ in probability as $n_p \wedge n_q \rightarrow \infty$. Then we analyze these conditions through several propositions.

Assumption 1. $\boldsymbol{\delta}^*$, which is the minimizer of (2) is unique.

Since (2) is convex and continuously differentiable with respect to $\boldsymbol{\delta}$, the above assumption is equivalent to stating the Hessian of (3) is positive definite for all $\boldsymbol{\delta}$.

Theorem 1. Suppose Assumption 1 holds,

$$\exists R_1 > 0, \|\nabla_{\boldsymbol{\delta}} \ell(\boldsymbol{\delta}^*)\| \leq \frac{R_1}{\sqrt{n_p \wedge n_q}}, \quad (6)$$

with probability at least ϵ_{R_1} and $\exists R_2 > 0, C_r > 1$,

$$\inf_{\boldsymbol{\delta} \in \Delta_n} \lambda_{\min} [\nabla_{\boldsymbol{\delta}}^2 \ell(\boldsymbol{\delta})] > R_2, \Delta_n := S\left(\boldsymbol{\delta}^*, \frac{R_1}{R_2} \cdot \frac{C_r}{\sqrt{n_p \wedge n_q}}\right), \quad (7)$$

with probability at least $1 - \epsilon_{R_2}$. Then $\exists N$ such that $n_p \wedge n_q > N$, we have $\hat{\boldsymbol{\delta}} \xrightarrow{\mathbb{P}} \boldsymbol{\delta}^*$ with probability $1 - \epsilon_{R_1} - \epsilon_{R_2}$.

Proof. Let us begin by considering the following constrained optimization problem:

$$\check{\boldsymbol{\delta}} := \operatorname{argmin}_{\boldsymbol{\delta} \in \Delta_n} \ell(\boldsymbol{\delta}; Z_p, Z_q). \quad (8)$$

The Lagrangian of (8) is:

$$\operatorname{Lag}(\mu, \boldsymbol{\delta}) := \ell(\boldsymbol{\delta}) + \mu \cdot \|\boldsymbol{\delta}^* - \boldsymbol{\delta}\| - \mu \cdot \frac{C_r}{\sqrt{n_p \wedge n_q}}.$$

The KKT condition states that the minimizer $\check{\boldsymbol{\delta}}$ must satisfy $\mathbf{0} = \nabla_{\boldsymbol{\delta}} \ell(\check{\boldsymbol{\delta}}) + \hat{\mu} \cdot \frac{\boldsymbol{\delta}^* - \check{\boldsymbol{\delta}}}{\|\boldsymbol{\delta}^* - \check{\boldsymbol{\delta}}\|}$ for some $\hat{\mu} \geq 0$. Rewrite this equality by expanding $\nabla_{\boldsymbol{\delta}} \ell(\check{\boldsymbol{\delta}})$ at $\boldsymbol{\delta}^*$ using mean value theorem in a coordinate-wise fashion:

$$\mathbf{0} = \nabla_{\boldsymbol{\delta}} \ell(\boldsymbol{\delta}^*) + \left[\nabla_{\boldsymbol{\delta}}^2 \ell(\bar{\boldsymbol{\delta}}) + \frac{\hat{\mu}}{\|\boldsymbol{\delta}^* - \check{\boldsymbol{\delta}}\|} \mathbf{I} \right] [\boldsymbol{\delta}^* - \check{\boldsymbol{\delta}}].$$

Note $\bar{\delta}_i := h\hat{\delta}_i + (1-h)\delta_i^*$ for some $h \in [0, 1]$ which implies $(\bar{\delta}_i - \delta_i^*)^2 = h^2(\hat{\delta}_i - \delta_i^*)^2 \leq (\hat{\delta}_i - \delta_i^*)^2$. Therefore, $\bar{\boldsymbol{\delta}} \in \Delta_n$.

After some algebra and using the fact that $\bar{\boldsymbol{\delta}} \in \Delta_n$ we get

$$\begin{aligned} \|\boldsymbol{\delta}^* - \check{\boldsymbol{\delta}}\| &= \left\| \left[\nabla_{\boldsymbol{\delta}}^2 \ell(\bar{\boldsymbol{\delta}}) + \frac{\hat{\mu}}{\|\boldsymbol{\delta}^* - \check{\boldsymbol{\delta}}\|} \mathbf{I} \right]^{-1} \nabla_{\boldsymbol{\delta}} \ell(\boldsymbol{\delta}^*) \right\| \\ &< \left\| [\nabla_{\boldsymbol{\delta}}^2 \ell(\bar{\boldsymbol{\delta}})]^{-1} \right\| \cdot \|\nabla_{\boldsymbol{\delta}} \ell(\boldsymbol{\delta}^*)\| \\ &\leq \frac{1}{R_2} \cdot \|\nabla_{\boldsymbol{\delta}} \ell(\boldsymbol{\delta}^*)\| \leq \frac{R_1}{R_2} \cdot \frac{1}{\sqrt{n_p \wedge n_q}} \end{aligned}$$

where the second line is due to Holder's inequality and the first inequality in the third line uses an equality $\|\mathbf{A}^{-1}\| = 1/\lambda_{\min}(\mathbf{A})$, if \mathbf{A} is p.s.d., then applying inequality (7). The last inequality in the third line is due to (6).

(6) holds with probability at least $1 - \epsilon_{R_1}$ and (7) holds with probability at least $1 - \epsilon_{R_2}$. A union bound shows the above inequality holds with probability at least $1 - \epsilon_{R_1} - \epsilon_{R_2}$.

Since the spherical constraint has radius $\frac{R_1}{R_2} \cdot \frac{C_r}{\sqrt{n_p \wedge n_q}}$ and $C_r > 1$, we conclude the minimizer $\check{\boldsymbol{\delta}}$ is in the interior of Δ_n with probability at least $1 - \epsilon_{R_1} - \epsilon_{R_2}$. The KKT condition also states, $\exists \hat{\mu} \geq 0, \hat{\mu} \cdot \left(\|\boldsymbol{\delta}^* - \check{\boldsymbol{\delta}}\| - \frac{R_1}{R_2} \cdot \frac{C_r}{\sqrt{n_p \wedge n_q}} \right) = 0$. Knowing $\check{\boldsymbol{\delta}}$ is in the interior of Δ_n , we can deduce $\hat{\mu} = 0$, which means the constraint $\boldsymbol{\delta} \in \Delta_n$ is inactive, so $\hat{\boldsymbol{\delta}} = \check{\boldsymbol{\delta}}$ with probability at least $1 - \epsilon_{R_1} - \epsilon_{R_2}$.

The fact that $\check{\boldsymbol{\delta}}$ is in the interior of a $\boldsymbol{\delta}^*$ -centered sphere whose radius shrinks at the rate $\frac{1}{\sqrt{n_p \wedge n_q}}$ with probability at least $1 - \epsilon_{R_1} - \epsilon_{R_2}$ allows us to conclude that $\check{\boldsymbol{\delta}} \xrightarrow{\mathbb{P}} \boldsymbol{\delta}^*$. Finally $\hat{\boldsymbol{\delta}} \xrightarrow{\mathbb{P}} \boldsymbol{\delta}^*$ due to $\hat{\boldsymbol{\delta}} = \check{\boldsymbol{\delta}}$ as discussed above. \square

3.2 Eigenvalue Lowerbound of $\nabla_{\boldsymbol{\delta}}^2 \ell(\boldsymbol{\delta})$

It is worth investigating condition (7) in Theorem 1, which states that the minimum eigenvalue of $\nabla_{\boldsymbol{\delta}}^2 \ell(\boldsymbol{\delta})$ is lower-bounded within the neighbourhood of $\boldsymbol{\delta}^*$. It is reasonable to assume that if the radius of Δ_n is small enough, $\inf_{\boldsymbol{\delta} \in \Delta_n} \lambda_{\min} [\nabla_{\boldsymbol{\delta}}^2 \ell(\boldsymbol{\delta})] \approx \lambda_{\min} [\nabla_{\boldsymbol{\delta}}^2 \ell(\boldsymbol{\delta}^*)]$. Indeed, Wely's inequality allows us to lower-bound $\inf_{\boldsymbol{\delta} \in \Delta_n} \lambda_{\min} [\nabla_{\boldsymbol{\delta}}^2 \ell(\boldsymbol{\delta})]$:

$$\begin{aligned} &\inf_{\boldsymbol{\delta} \in \Delta_n} \lambda_{\min} [\nabla_{\boldsymbol{\delta}}^2 \ell(\boldsymbol{\delta})] \\ &\geq \lambda_{\min} [\nabla_{\boldsymbol{\delta}}^2 \ell(\boldsymbol{\delta}^*)] - \sup_{\boldsymbol{\delta} \in \Delta_n} \|\nabla_{\boldsymbol{\delta}}^2 \ell(\boldsymbol{\delta}^*) - \nabla_{\boldsymbol{\delta}}^2 \ell(\boldsymbol{\delta})\|. \end{aligned} \quad (9)$$

Given $\nabla_{\delta}^2 \ell(\delta)$ is smooth and if Δ_n is small enough, we have $\nabla_{\delta}^2 \ell(\delta^*) \approx \nabla_{\delta}^2 \ell(\delta)$. Thus $\lambda_{\min} [\nabla_{\delta}^2 \ell(\delta)]$ should be the dominating term in (9). This claim will be verified later via numerical experiments in Section 7.1.

In practice, δ^* is unknown. However, in many applications, we always assume that $p(\mathbf{z}|X_p)$ is very similar to $q(\mathbf{z}|X_q)$, so we can further assume that δ^* is close to zero as a result of the mildness of the posterior ratio function. Thus, we can verify (7) in a larger neighbourhood of $\mathbf{0}$ which should automatically cover the true Δ_n .

3.3 Convergence of $\nabla_{\delta} \ell(\delta^*)$

Now we analyze the condition (6) which states $\nabla_{\delta} \ell(\delta^*)$ should converge to zero in terms of ℓ_2 norm at the rate $\frac{1}{\sqrt{n_p \wedge n_q}}$.

For simplicity, we define two weighting functions:

$$w_p(\mathbf{z}) := \frac{l_p(\mathbf{z})}{\hat{p}(X_p)}, w_q(\mathbf{z}; \delta) := \frac{l_q(\mathbf{z}) \exp\langle \delta^\top \mathbf{f}(\mathbf{z}) \rangle}{\hat{\mathbb{E}}_{q\mathbf{z}} [l_q(\mathbf{z}) \cdot \exp\langle \delta^\top \mathbf{f}(\mathbf{z}) \rangle]}.$$

The following proposition shows the gradient can be decomposed into two parts.

Proposition 2. *The gradient of $\ell(\delta^*)$ can be written as*

$$\begin{aligned} \frac{-\nabla_{\delta} \ell(\delta^*)}{\hat{p}(X_p)} &= \mathbf{a} + \mathbf{b}. \\ \mathbf{a} &:= \hat{\mathbb{E}}_{p\mathbf{z}} [w_p(\mathbf{z}) \mathbf{f}(\mathbf{z})] - \mathbb{E}_{p\mathbf{z}} \left[\frac{l_p(\mathbf{z})}{p(X_p)} \mathbf{f}(\mathbf{z}) \right] \\ \mathbf{b} &:= \mathbb{E}_{q\mathbf{z}} \left[\frac{l_q(\mathbf{z}) r(\mathbf{z}; \delta^*)}{q(X_q)} \mathbf{f}(\mathbf{z}) \right] - \hat{\mathbb{E}}_{q\mathbf{z}} [w_q(\mathbf{z}; \delta^*) \mathbf{f}(\mathbf{z})]. \end{aligned}$$

Proof. First, by definition

$$\frac{-\nabla_{\delta} \ell(\delta^*)}{\hat{p}(X_p)} = \hat{\mathbb{E}}_{p\mathbf{z}} [w_p(\mathbf{z}) \mathbf{f}(\mathbf{z})] - \hat{\mathbb{E}}_{q\mathbf{z}} [w_q(\mathbf{z}; \delta^*) \mathbf{f}(\mathbf{z})]$$

Furthermore, δ^* is the optimal parameter of (2) so the optimality condition (4) implies

$$\mathbb{E}_{q\mathbf{z}} \left[\frac{l_q(\mathbf{z}) r(\mathbf{z}; \delta^*)}{q(X_q)} \mathbf{f}(\mathbf{z}) \right] = \mathbb{E}_{p\mathbf{z}} \left[\frac{l_p(\mathbf{z})}{p(X_p)} \mathbf{f}(\mathbf{z}) \right].$$

Combining above two equalities gives desired results in Proposition 2. \square

Upon inspection, we can see both \mathbf{a} and \mathbf{b} are differences between an expectation and a weighted sum where the weighting functions are themselves approximated using prior samples.

Proving the convergence of $\nabla_{\delta} \ell(\delta^*)$ would require further regularity conditions. To keep our paper uncluttered, we provide a general rationale toward proving this statement.

Due to triangle inequality, \mathbf{a} is upper-bounded by:

$$\|\mathbf{a}\| \leq \frac{1}{\hat{p}(X_p)} \left\| \hat{\mathbb{E}}_{p\mathbf{z}} [l_p(\mathbf{z}) \mathbf{f}(\mathbf{z})] - \mathbb{E}_{p\mathbf{z}} [l_p(\mathbf{z}) \mathbf{f}(\mathbf{z})] \right\| + \frac{|p(X_p) - \hat{p}(X_p)|}{p(X_p) \cdot \hat{p}(X_p)} \cdot \|\mathbb{E}_{p\mathbf{z}} [l_p(\mathbf{z}) \mathbf{f}(\mathbf{z})]\|.$$

Then concentration inequalities can be used to derive the rate at which RHS converges to zero. Under certain regularity conditions, we can expect a convergence rate $\frac{1}{\sqrt{n_p}}$. By imposing similar assumptions and using a similar argument, we can obtain the $\frac{1}{\sqrt{n_q}}$ convergence rate for \mathbf{b} . Thus $\|\nabla_{\delta} \ell(\delta^*)\|$ converges to zero at a slower rate between $\frac{1}{\sqrt{n_p}}$ and $\frac{1}{\sqrt{n_q}}$ with high probability.

4 Asymptotic Normality of $\hat{\boldsymbol{\delta}}$

In this section, we show the normality of the estimator (5). Let us define a few notations $\mathbf{H}_q = \mathbb{E}_{qz} [\nabla_{\boldsymbol{\delta}}^2 \ell(\boldsymbol{\delta}^*)]$, $\boldsymbol{\Sigma}_p = \text{Var}_{pz} [w_p(\mathbf{z}) \mathbf{f}(\mathbf{z})]$, $\boldsymbol{\Sigma}_q = \text{Var}_{qz} [w_q(\mathbf{z}; \boldsymbol{\delta}^*) \mathbf{f}(\mathbf{z})]$.

Theorem 2. *If $\hat{\boldsymbol{\delta}} \xrightarrow{\mathbb{P}} \boldsymbol{\delta}^*$ and*

$$\sup_{\boldsymbol{\delta} \in \Delta_n} \|\nabla_{\boldsymbol{\delta}}^2 \ell(\boldsymbol{\delta}) - \mathbb{E}_{qz} [\nabla_{\boldsymbol{\delta}}^2 \ell(\boldsymbol{\delta})]\| \xrightarrow{\mathbb{P}} 0, \quad (10)$$

then

$$\frac{\sqrt{n_p} [\boldsymbol{\delta}^* - \hat{\boldsymbol{\delta}}]}{\hat{p}(X_p)} \rightsquigarrow \mathcal{N} \left[\mathbf{0}, \mathbf{H}_q^{-1} \left(\boldsymbol{\Sigma}_p + \frac{n_p}{n_q} \cdot \boldsymbol{\Sigma}_q \right) \mathbf{H}_q^{-1} \right]. \quad (11)$$

In practice, we can use $\hat{\boldsymbol{\delta}}$ to replace $\boldsymbol{\delta}^*$ and use sample average to replace expectations when calculating the above asymptotic variance. We list (10) as an assumption and do not prove it in this paper since proving uniform convergence requires further regularity conditions. We only establish asymptotic results in this paper.

Proof. This theorem is the consequence of the estimation equation of (5):

$$\mathbf{0} = \nabla_{\boldsymbol{\delta}} \ell(\hat{\boldsymbol{\delta}}) = \nabla_{\boldsymbol{\delta}} \ell(\boldsymbol{\delta}^*) + \nabla_{\boldsymbol{\delta}}^2 \ell(\bar{\boldsymbol{\delta}}) [\boldsymbol{\delta}^* - \hat{\boldsymbol{\delta}}],$$

where the last line is due to mean value theorem. Thus,

$$\begin{aligned} -\nabla_{\boldsymbol{\delta}} \ell(\boldsymbol{\delta}^*) &= \nabla_{\boldsymbol{\delta}}^2 \ell(\bar{\boldsymbol{\delta}}) [\boldsymbol{\delta}^* - \hat{\boldsymbol{\delta}}] \\ -\nabla_{\boldsymbol{\delta}} \ell(\boldsymbol{\delta}^*) &= [\mathbf{H}_q + o_p(1)] [\boldsymbol{\delta}^* - \hat{\boldsymbol{\delta}}], \end{aligned}$$

where the last line is due to (10) and continuous mapping theorem.

Therefore

$$\frac{[\hat{\boldsymbol{\delta}} - \boldsymbol{\delta}^*]}{\hat{p}(X_p)} = [\mathbf{H}_q + o_p(1)]^{-1} \frac{\nabla_{\boldsymbol{\delta}} \ell(\boldsymbol{\delta}^*)}{\hat{p}(X_p)}. \quad (12)$$

Proposition 2 states that $\frac{-\nabla_{\boldsymbol{\delta}} \ell(\boldsymbol{\delta}^*)}{\hat{p}(X_p)} = \mathbf{a} + \mathbf{b}$.

Since X_p, X_q and $\mathbf{z}_p, \mathbf{z}_q$ are independent of each other, $\frac{\nabla_{\boldsymbol{\delta}} \ell(\boldsymbol{\delta}^*)}{\hat{p}(X_p)}$ is the sum of two *independent* zero-mean random variables \mathbf{a} and \mathbf{b} with covariance $\boldsymbol{\Sigma}_p$ and $\boldsymbol{\Sigma}_q$ respectively.

Applying CLT on $\sqrt{n_p} \mathbf{a}$ and $\sqrt{n_q} \mathbf{b}$ yields $\frac{-\nabla_{\boldsymbol{\delta}} \ell(\boldsymbol{\delta}^*)}{\hat{p}(X_p)} \rightsquigarrow \mathcal{N}(\mathbf{0}, \boldsymbol{\Sigma}_p + \frac{n_p}{n_q} \boldsymbol{\Sigma}_q)$. Finally, (12) indicates that we should left and right multiply the covariance by \mathbf{H}_q^{-1} to obtain covariance of $\frac{\sqrt{n_p} \cdot (\boldsymbol{\delta}^* - \hat{\boldsymbol{\delta}})}{\hat{p}(X_p)}$. This yields desired results in (11). \square

5 Dual Estimator of (5)

Instead of (5), we can consider an alternative estimator:

$$\begin{aligned} \hat{\boldsymbol{\delta}}' &:= \underset{\boldsymbol{\delta}}{\text{argmin}} E_{n_q}(\boldsymbol{\delta}), \\ E_{n_q}(\boldsymbol{\delta}) &:= \left\| \hat{p}(X_p) \hat{\mathbb{E}}_q [w_q(\mathbf{z}; \boldsymbol{\delta}) \mathbf{f}(\mathbf{z})] - \sum_{i=1}^{n_q} \hat{\mu}_i \mathbf{f}(\mathbf{z}_q^{(i)}) \right\|, \end{aligned}$$

where

$$\begin{aligned}
\hat{\boldsymbol{\mu}} &:= \operatorname{argmin}_{\boldsymbol{\mu} \geq 0} \sum_{i=1}^{n_q} \mu_i \log \mu_i - \mu_i \log l_q(\mathbf{z}_q^{(i)}) \\
\text{s.t. : } &\left\| \hat{\mathbb{E}}_{p_{\mathbf{z}}} [l_p(\mathbf{z}) \mathbf{f}(\mathbf{z})] - \sum_{i=1}^{n_q} \mu_i \mathbf{f}(\mathbf{z}_q^{(i)}) \right\| \leq R_n \\
&\sum_i \mu_i = \hat{p}(X_p),
\end{aligned} \tag{13}$$

and R_n is a constant. (13) is derived from the *Lagrangian dual* of (5). A poof can be found in the supplementary material.

Theorem 3. *Suppose Assumption 1 holds, $E_{n_q}(\hat{\boldsymbol{\delta}}') \leq C_0$, (6) holds with probability at least $1 - \epsilon_{R_1}$ and $\exists R_2 > 0, R_3 \geq 0, C_r > 1$,*

$$\begin{aligned}
&\inf_{\boldsymbol{\delta} \in \Delta_n} \lambda_{\min} [\nabla_{\boldsymbol{\delta}}^2 \ell(\boldsymbol{\delta})] > R_2, \\
\Delta_n &:= \mathbb{S} \left(\boldsymbol{\delta}^*, \frac{R_1 + R_3}{R_2} \frac{C_r}{\sqrt{n_p \wedge n_q}} + \frac{C_0}{R_2} \right),
\end{aligned} \tag{14}$$

with probability at least ϵ_{R_2} , then $\exists R_n \leq \frac{R_3}{\sqrt{n_p \wedge n_q}}$ such that $\|\boldsymbol{\delta}^ - \hat{\boldsymbol{\delta}}'\| \leq \frac{R_1 + R_3}{R_2} \frac{1}{\sqrt{n_p \wedge n_q}} + \frac{C_0}{R_2}$ with probability at least $1 - \epsilon_{R_1} - \epsilon_{R_2}$.*

The proof can be found in Section 12 in the supplementary material. In our experiments, we find E_{n_q} , which can be easily calculated, is around 10^{-7} . Therefore, in practice, $C_0 \approx 0$.

This formulation is particularly useful when \mathbf{f} and $\boldsymbol{\delta}$ are in Reproducing Kernel Hilbert Space (RKHS) Scholkopf and Smola ((2001)) as \mathbf{f} only appears inside the norm which can be evaluated using the inner product.

6 Related Works

Density Ratio Estimation. DRE approximates the ratio function between two probability density functions given two sets of samples, which are drawn from these two distributions. PRE is closely related to a DRE method called KLIEP. Indeed, if we let $l_p = 1$ and $l_q = 1$, then $\hat{\boldsymbol{\delta}}$ becomes the KLIEP estimator of $\frac{p(\mathbf{z})}{q(\mathbf{z})}$. However, an important difference between DRE and PRE is that while DRE treats observations in X_p and X_q as variables, PRE treats them as constants which are only used for calculating $l_p(\mathbf{z})$ and $l_q(\mathbf{z})$. Thus, PRE is fundamentally different from calculating the density ratio function using X_p and X_q .

(Implicit) Variational Inference. The optimization of PRE and VI both minimizes a KL divergence:

$$\text{VI : } \min_{\boldsymbol{\theta}} \text{KL}[q_{\boldsymbol{\theta}} | l_p p_{\mathbf{z}}] \quad \text{PRE : } \min_{\boldsymbol{\delta}} \text{KL}[l_p p_{\mathbf{z}} | l_q q_{\mathbf{z}} r_{\boldsymbol{\delta}}].$$

Despite such a similarity, VI and PRE have very different goals: VI approximates a posterior from *one* set of observation and parameterizes a posterior model, while PRE approximates the posterior ratio function from *two* sets of data and parameterizes a posterior *ratio* model.

Recent attempts to incorporate DRE into VI used individual samples from $X_p, Z_q | X_p$, and Z_p Huszár ((2017)); Shi et al. ((2018)). Huszár proposed to estimate the ratio term $\frac{q_{\boldsymbol{\theta}}(\mathbf{z} | X_p)}{p(\mathbf{z})}$ in the Evidence Lower Bound using DRE objectives as a middle step. However, no ratio model is introduced. Both approaches require the ability to sample from $q(\mathbf{z} | X_p)$ and the final targets are still learning parameter $\boldsymbol{\theta}$.

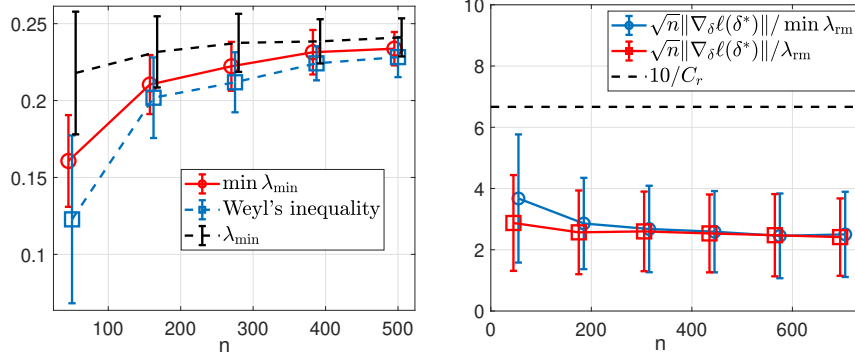


Figure 1: Numerical evaluation of Theorem 1's conditions

7 Numerical Experiments

7.1 Conditions for Consistency

In the first experiment, we numerically evaluate the conditions required by Theorem 1 and explore possible settings of the constants in this theorem.

We let $X_p = X_q = [0, 0]$, $l_p = l_q = \mathcal{N}_X(\mathbf{z}, \mathbf{I})$, $\mathbf{z} \in \mathbb{R}^2$ and Z_p, Z_q be independently samples from a 2 dimensional standard normal distribution. $n_p = n_q = n$. We use $\mathbf{f}(\mathbf{z}) = \mathbf{z}$ in our posterior ratio model and it can be seen that $\delta^* = \mathbf{0}$ by our construction of the dataset.

We first investigate the minimum eigenvalue condition on $\nabla_{\delta}^2 \ell(\delta)$. In the left plot of Figure 1, we plot $\min_{\delta \in \Delta_n} \lambda_{\min} [\nabla_{\delta}^2 \ell(\delta)]$ (which is obtained by numerical optimization) as a red solid line. Here $\Delta_n := \mathcal{S}(\mathbf{0}, \frac{10}{\sqrt{n}})$ and the error bar indicates the standard deviation of 50 runs. It can be seen that when $n \geq 400$, $\min_{\delta \in \Delta_n} \lambda_{\min} [\nabla_{\delta}^2 \ell(\delta)]$ minus two standard deviation is safely bounded by 0.18 from below.

We also investigate the tightness a lower-bound obtained from Wye'l's inequality (see (9)) which is marked by a blue dash line. As we can see, when $n \geq 400$, Wye'l's inequality becomes very close to $\min_{\delta \in \Delta_n} \lambda_{\min} [\nabla_{\delta}^2 \ell(\delta)]$ and consequently $\lambda_{\min} [\nabla_{\delta}^2 \ell(\delta^*)]$ (black dash line) becomes a good approximation to $\min_{\delta \in \Delta_n} \lambda_{\min} [\nabla_{\delta}^2 \ell(\delta)]$.

Now we explore some possible settings of the constants in Theorem 1. It can be seen from Theorem 1 that R_1 and R_2 determine ϵ_{R_1} and ϵ_{R_2} . To make probability $1 - \epsilon_{R_1} - \epsilon_{R_2}$ as large as possible, we should make R_1 large but R_2 small. However, if the ratio R_1/R_2 is large, Δ_n would be large too ($C_r > 1$) and condition (7) may struggle to hold. To investigate the possible settings of R_1 and R_2 , we plot $\frac{\|\sqrt{n} \nabla_{\delta} \ell(\delta^*)\|}{\inf_{\delta \in \Delta_n} \lambda_{\min} [\nabla_{\delta}^2 \ell(\delta)]}$ in the right plot of Figure 1, where Δ_n has a radius $10/\sqrt{n}$. The plot is generated from 500 repetitions with different draws of samples from $p(\mathbf{z}), q(\mathbf{z})$. Error bars indicate standard deviations. We choose $C_r = 1.5$.

Since the ratio $\frac{\|\sqrt{n} \nabla_{\delta} \ell(\delta^*)\|}{\inf_{\delta \in \Delta_n} \lambda_{\min} [\nabla_{\delta}^2 \ell(\delta)]} \leq \frac{R_1}{R_2} = 10/C_r$, 6.66 is the upper limit of $\frac{\|\sqrt{n} \nabla_{\delta} \ell(\delta^*)\|}{\inf_{\delta \in \Delta_n} \lambda_{\min} [\nabla_{\delta}^2 \ell(\delta)]}$. The plot shows, this requirement is comfortably met with some room to spare. We can see that the averaged ratio plus two standard deviations is nicely bounded by $10/C_r$ from above.

We can also see from this plot that $\frac{\|\sqrt{n} \nabla_{\delta} \ell(\delta^*)\|}{\lambda_{\min} [\nabla_{\delta}^2 \ell(\delta^*)]}$ becomes a nice approximation to $\frac{\|\sqrt{n} \nabla_{\delta} \ell(\delta^*)\|}{\inf_{\delta \in \Delta_n} \lambda_{\min} [\nabla_{\delta}^2 \ell(\delta)]}$ when n is larger than 400, which aligns with our expectation in Section 3.2 that $\nabla_{\delta}^2 \ell(\delta^*) \approx \nabla_{\delta}^2 \ell(\delta)$, $\forall \delta \in \Delta_n$ when n is large.

7.2 Asymptotic Normality of $\hat{\delta}$

In this experiment, we validate the asymptotic distribution discussed in Section 4 under a finite-sample setting.

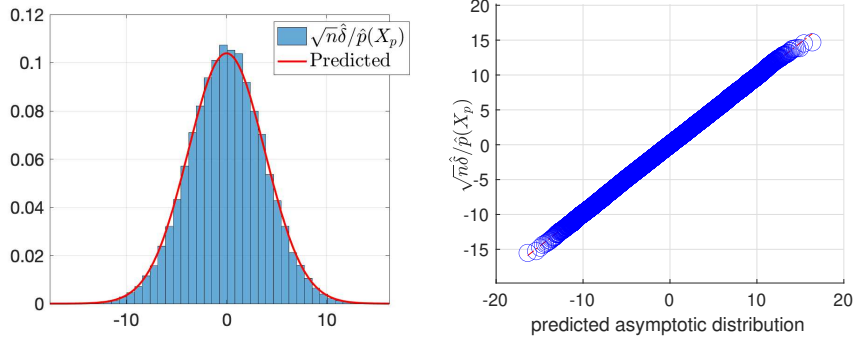


Figure 2: Simulation vs. Theorem 2's prediction

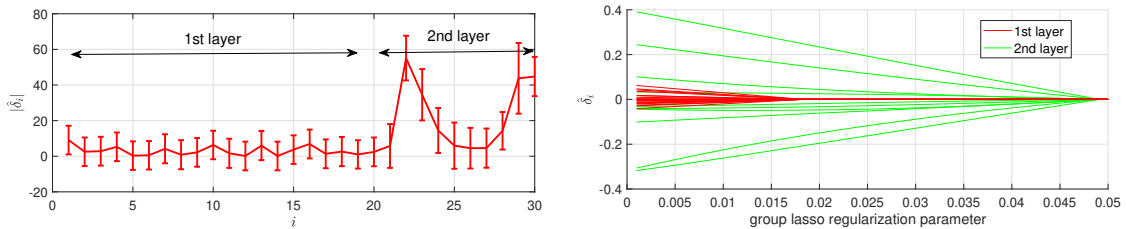


Figure 3: Comparing Two Neural Networks

We generate two sets of 100 random samples independently as X_p and X_q from a normal distribution $\mathcal{N}(0.5, 0.1^2)$ and set the likelihood function $l_p(z) = l_q(z) := \mathcal{N}_X(z \cdot \mathbf{1}, 8^2 \cdot \mathbf{I})$, where $\mathbf{1}$ is a 100-dimensional vector filled with ones and \mathbf{I} is an 100×100 identity matrix. 500 prior samples Z_p and Z_q are independently drawn from $p(z) = q(z) = \mathcal{N}(0, 1)$. $n_p = n_q = n$, $f(z) = z$. Then $\hat{\delta}$ is calculated using (5) given Z_p, Z_q, X_p, X_q, l_p and l_q .

We run the simulation of $\hat{\delta}$ 50000 times with different random seeds and plot the histogram of $\sqrt{n}\hat{\delta}/\hat{p}(X_p)$ in Figure 2. Theorem 2 predicted asymptotic distribution of $\sqrt{n}[\hat{\delta} - \delta^*]/\hat{p}(X_p)$ with $\delta^* = 0$ is plotted as a red solid line over the histogram calculated from a *single run*. These two distributions are also compared on the quantile quantile plot (qq-plot) in Figure 2.

Note that in this experiment, $p(z|X_p) \neq q(z|X_q)$ since $X_p \neq X_q$. However, as we take 100 samples from the same distribution as X_p and X_q , given this strong evidence, the posterior should be very close to each other. Thus Theorem 2 should be applicable. Both plots show that the prediction made by Theorem 2 matches the simulations well.

8 Application: Interpretable Comparison between Two Neural Nets

Comparing different neural nets is a challenging task. The optimization of neural net is non-convex: two networks with the same structure may achieve the same predicting performance but have completely different sets of parameters.

By following the idea of Bayesian neural nets, (see e.g. Gal and Ghahramani ((2016)); Blundell et al. ((2015))), we can treat parameters of a network as random variables. Therefore the differences between two nets can be characterized by the posterior ratio $\frac{p(\mathbf{z}|X_p)}{q(\mathbf{z}|X_q)}$ where \mathbf{z} are parameters and X_p and X_q are datasets on which two neural nets are evaluated.

Good priors for Bayesian neural nets are hard to come by, particularly for a large network. In this work, we initialize the neural net with different random parameters drawn from a normal distribution with zero mean and standard deviation 0.1, then we run stochastic gradient descent for one iteration and extract the updated parameters as a prior sample \mathbf{z} . We find the prior samples obtained in this way are much more informative than simple random draws from naive priors. Although we will not have an explicit expression for such a prior, it is *not* a requirement for our posterior ratio estimation. This pre-training dataset is independent of X_p or X_q .

In this experiment, we use a posterior ratio model $r(\mathbf{z}; \boldsymbol{\delta}) \propto \exp[\boldsymbol{\delta}^\top \mathbf{f}(\mathbf{z})]$, where $\mathbf{f}(\mathbf{z}) := [\mathbf{f}_1(\mathbf{z}_1), \mathbf{f}_2(\mathbf{z}_2) \cdots]^\top$. \mathbf{f}_i is the output of the hidden units at i -th layer. For example, a [784, 20, 10] neural net will have $\mathbf{f}_1 \in \mathbb{R}^{20}$ and $\mathbf{f}_2 \in \mathbb{R}^{10}$.

We select the entire training portion of the MNIST dataset as the pre-training dataset. The neural network is constructed as [784,20,10], where 784 and 10 corresponds to the data dimension and the output dimension. 20000 pre-trained \mathbf{z} are obtained and we use the first 10000 sample as Z_p and the later half as Z_q . $\log l_p(\mathbf{z})$, $\log l_q(\mathbf{z})$ are the negative logistic-loss functions computed on X_p and X_q respectively.

We set X_p to be the dataset containing digits '2' and '3' and X_q to be digits '9' and '0'. The estimated $|\sqrt{n}\hat{\boldsymbol{\delta}}|$ is plotted in Figure 3 and the 2 times the asymptotic standard deviations predicted by Theorem 2 is plotted as the errorbars. It can be seen that almost all the outputs from the 1st layer hidden units does not seem to contribute to the change as the corresponding $\hat{\delta}_i$ are close to 0. However, when it comes to the second layer, we found some latent units outputs are significantly larger than 0, for example, the outputs with indices 2, 3 and 9, 10. This coincides with the fact that X_p contains digits 2 and 3 while X_q contains digits 9 and 10. This result also shows that the outputs of the first layer of hidden units seem to be invariant to the dataset change.

To further verify this, we use group lasso penalty together with (5): the lasso penalty are applied on elements in $\boldsymbol{\delta}$, which are grouped according to the output layer: $[\delta_1 \cdots \delta_{20}]$ is group one and $[\delta_{21} \cdots \delta_{30}]$ is group two. The regularization path of $\boldsymbol{\delta}$ is plotted in Figure 3. It can be seen that $[\delta_1 \cdots \delta_{20}]$ reduces to zero at an earlier stage than the $[\delta_{21} \cdots \delta_{30}]$. This verifies our observation earlier that the second layer of this neural network seems to be more sensitive to the change of datasets from X_p to X_q .

9 Application: Weighted Maximum a Posteriori

Maximum *a Posteriori* (MAP) is a common Bayesian estimation technique. In this section, let us consider a weighted MAP (WMAP) using the posterior ratio:

$$\hat{\mathbf{z}} = \underset{\mathbf{z}}{\operatorname{argmax}} q(\mathbf{z}|X_q) \cdot r(\mathbf{z}; \hat{\boldsymbol{\delta}}), \quad (15)$$

where $r(\mathbf{z}; \hat{\boldsymbol{\delta}})$ is an estimate of the posterior ratio $\frac{p(\mathbf{z}|X_p)}{q(\mathbf{z}|X_q)}$ and X_p and X_q are two observations. We use this as a replacement of the MAP $\mathbf{z}_{\text{MAP}} = \underset{\mathbf{z}}{\operatorname{argmax}} p(\mathbf{z}|X_p)$. We drop the normalizing term $Z(\boldsymbol{\delta})$ in $r(\mathbf{z}; \boldsymbol{\delta})$ since it is not a function of \mathbf{z} . Taking the logarithm, (15) can be transformed into

$$\hat{\mathbf{z}} = \underset{\mathbf{z}}{\operatorname{argmax}} \log q(\mathbf{z}|X_q) + \hat{\boldsymbol{\delta}}^\top \mathbf{f}(\mathbf{z}).$$

In some cases, evaluating the likelihood function $l_p(\mathbf{z})$ or its gradient may be computationally expensive, which makes classic MAP slow. However, if we can approximate l_p using a much less computationally demanding likelihood l_q and the model of ratio is simple enough, say $r(\mathbf{z}; \boldsymbol{\delta}) \propto \exp(\boldsymbol{\delta}^\top \mathbf{z})$, then (15) can be used for fast MAP approximation.

We apply WMAP to a shear building stiffness estimation problem. Specifically, we estimate the floor stiffness using readings of an accelerometer installed on the top floor of a multi-story building with d stiffness parameters Behmanesh et al. ((2017)); Yan and Katafygiotis ((2015)). In this setting, the latent variable $\mathbf{z} \in [0, 1]^d$ is the stiffness of the building and the observation $X_p \in \mathbb{R}^d$ is the first d natural frequencies

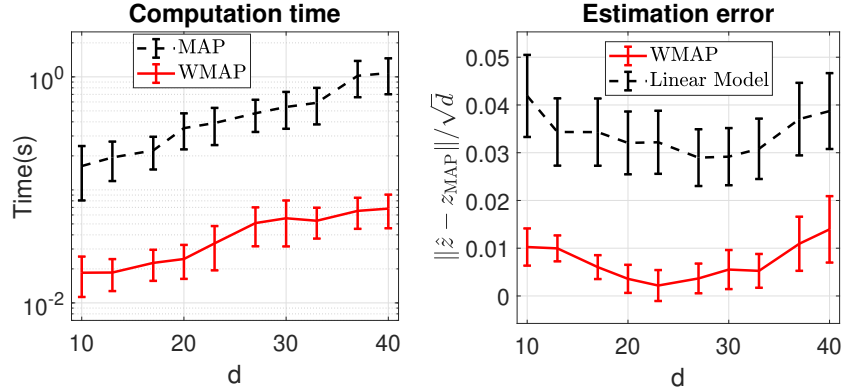


Figure 4: Approximate MAP for floor stiffness estimation.

derived from accelerometer readings. The likelihood function is given by $p(X_p|\mathbf{z}) = \mathcal{N}_{X_p}(\boldsymbol{\xi}(\mathbf{z}), \sigma^2 \mathbf{I}_d)$ where σ^2 is pre-determined by heuristics. $\boldsymbol{\xi}$ is a Finite Element model and is governed by a second order differential equation Simoen et al. ((2015)). It can be expensive to evaluate Cheung and Beck ((2009)). We approximate $p(X_p|\mathbf{z})$ via a naive linear Gaussian model $q(X_p|\mathbf{z}) = \mathcal{N}_{X_p}(\hat{\boldsymbol{\beta}} \circ \mathbf{z}, \sigma^2)$, where \circ means element-wise product and $\hat{\boldsymbol{\beta}}$ is obtained by minimizing $\sum_i \|\boldsymbol{\xi}(\mathbf{z}_i) - \boldsymbol{\beta} \circ \mathbf{z}_i\|^2$ for 15 pre-selected \mathbf{z}_i . This is an independent, one-off procedure, and we do not need to perform it every time when we observe a new X_p .

Both $p(\mathbf{z})$ and $q(\mathbf{z})$ are d -dimensional truncated normal distribution with mean 1 and standard deviation 1 and the truncation domain is $[0, 1]^d$. The priors assign the highest belief to $\mathbf{1}$ because it is the most probable state for most new buildings. To compute the posterior ratio, 5000 samples are drawn from $p(\mathbf{z})$ and $q(\mathbf{z})$ respectively.

Figure 4 shows the comparison of computation time and estimation error. In the left figure, we compare the computation time between WMAP and classic MAP over 100 runs across $d = 10 \dots 40$. Error bars indicate standard deviations computed from results over 100 runs. WMAP computation time includes time for posterior ratio estimation *and* WMAP itself. The plot shows, WMAP is one order of magnitude faster than classic MAP on this problem despite having to solve posterior ratio estimation *and* MAP approximation. On the right hand side, we plot the difference between $\hat{\mathbf{z}}$ and true MAP solution \mathbf{z}_{MAP} (solid red curve). Standard deviations over 100 runs are plotted as error bars. The result shows, the difference between $\hat{\mathbf{z}}$ and \mathbf{z}_{MAP} is around 0.01 which is considered small given a $[0, 1]$ span. Moreover, WMAP achieves significantly lower estimation error than just using the linear model $q(X_p|\mathbf{z})$ and the prior $p(\mathbf{z})$ (dotted black curve).

10 Conclusions

In this paper, we study the problem of learning latent distribution changes via posterior ratio estimation. We propose a novel method that directly estimates the posterior ratio from two observed datasets, two likelihood functions and two sets of synthetic samples from priors. The proposed method is consistent and the estimated parameters has a normal distribution as the number of prior samples tending to infinity. The conditions of the consistent theorem and the asymptotic normality are verified under finite sample settings. We consider two practical applications for the posterior ratio: interpreting differences between two neural nets and fast approximation of a shear building stiffness estimation problem. Both experiments report promising results.

References

M. Arjovsky, S. Chintala, and L. Bottou. Wasserstein generative adversarial networks. In *Proceedings of the 34th International Conference on Machine Learning*, volume 70 of *Proceedings of Machine Learning*

- Research*, pages 214–223, 2017.
- I. Behmanesh, B. Moaveni, and C. Papadimitriou. Probabilistic damage identification of a designed 9-story building using modal data in the presence of modeling errors. *Engineering Structures*, 131:542–552, 2017.
- D. M. Blei, A. Kucukelbir, and J. D. McAuliffe. Variational inference: A review for statisticians. *Journal of the American Statistical Association*, 112(518):859–877, 2017.
- C. Blundell, J. Cornebise, K. Kavukcuoglu, and D. Wierstra. Weight uncertainty in neural network. In *Proceedings of the 32nd International Conference on Machine Learning*, volume 37 of *Proceedings of Machine Learning Research*, pages 1613–1622, 07–09 Jul 2015.
- S. H. Cheung and J. L. Beck. Bayesian model updating using hybrid monte carlo simulation with application to structural dynamic models with many uncertain parameters. *Journal of engineering mechanics*, 135(4): 243–255, 2009.
- C. Frogner, C. Zhang, H. Mobahi, M. Araya, and T. A. Poggio. Learning with a wasserstein loss. In *Advances in Neural Information Processing Systems*, pages 2053–2061, 2015.
- Y. Gal and Z. Ghahramani. Dropout as a bayesian approximation: Representing model uncertainty in deep learning. In *Proceedings of The 33rd International Conference on Machine Learning*, volume 48 of *Proceedings of Machine Learning Research*, pages 1050–1059, New York, New York, USA, 20–22 Jun 2016. PMLR.
- A. Genevay, M. Cuturi, G. Peyré, and F. Bach. Stochastic optimization for large-scale optimal transport. In *Advances in neural information processing systems*, pages 3440–3448, 2016.
- I. Goodfellow, J. Pouget-Abadie, M. Mirza, B. Xu, D. Warde-Farley, S. Ozair, A. Courville, and Y. Bengio. Generative adversarial nets. In *Advances in neural information processing systems 27*, pages 2672–2680, 2014.
- A. Gretton, K. M. Borgwardt, M. J. Rasch, B. Schölkopf, and A. Smola. A kernel two-sample test. *Journal of Machine Learning Research*, 13(Mar):723–773, 2012.
- F. Huszár. Variational inference using implicit distributions. *arXiv preprint arXiv:1702.08235*, 2017.
- Y. Kawahara and M. Sugiyama. Sequential change-point detection based on direct density-ratio estimation. *Statistical Analysis and Data Mining*, 5(2):114–127, 2012.
- S. Nowozin, B. Cseke, and R. Tomioka. f-gan: Training generative neural samplers using variational divergence minimization. In *Advances in Neural Information Processing Systems*, pages 271–279, 2016.
- J. Quionero-Candela, M. Sugiyama, A. Schwaighofer, and N. D. Lawrence. *Dataset shift in machine learning*. The MIT Press, 2009.
- B. Scholkopf and A. J. Smola. *Learning with kernels: support vector machines, regularization, optimization, and beyond*. MIT press, 2001.
- J. Shi, S. Sun, and Z. J. Kernel implicit variational inference. In *International Conference on Learning Representations*, 2018. URL <https://openreview.net/forum?id=r114eQWOZ>.
- E. Simoen, G. De Roeck, and G. Lombaert. Dealing with uncertainty in model updating for damage assessment: A review. *Mechanical Systems and Signal Processing*, 56:123–149, 2015.
- M. Sugiyama, T. Suzuki, S. Nakajima, H. Kashima, P. von Bünau, and M. Kawanabe. Direct importance estimation for covariate shift adaptation. *Annals of the Institute of Statistical Mathematics*, 60(4):699–746, 2008.

- M. Sugiyama, T. Suzuki, and T. Kanamori. *Density Ratio Estimation in Machine Learning*. Cambridge University Press, 2012a.
- M. Sugiyama, T. Suzuki, and T. Kanamori. Density-ratio matching under the Bregman divergence: a unified framework of density-ratio estimation. *Annals of the Institute of Statistical Mathematics*, 64(5):1009–1044, 2012b.
- Y. Tsuboi, H. Kashima, S. Hido, S. Bickel, and M. Sugiyama. Direct density ratio estimation for large-scale covariate shift adaptation. *Journal of Information Processing*, 17:138–155, 2009.
- W.-J. Yan and L. S. Katafygiotis. A novel bayesian approach for structural model updating utilizing statistical modal information from multiple setups. *Structural Safety*, 52:260–271, 2015.

11 The Dual Formulation of (13)

(5) can be re-written as

$$\begin{aligned} & \min_{\boldsymbol{\delta}, t_i} - \hat{\mathbb{E}}_{p_{\mathbf{z}}} [l_p(\mathbf{z}) \cdot \langle \boldsymbol{\delta}, \mathbf{f}(\mathbf{z}) \rangle] + \hat{p}(X_p) \cdot \log \hat{\mathbb{E}}_{q_{\mathbf{z}}} [l_q(\mathbf{z}) \exp(t)], \\ & \text{subject to } \forall i \in \{1 \dots n_q\}, t_i = \langle \boldsymbol{\delta}, \mathbf{f}(\mathbf{z}^{(i)}) \rangle. \end{aligned}$$

Write the Lagrangian of the above convex optimization,

$$\max_{\mu_i} \min_{\boldsymbol{\delta}, t_i} - \hat{\mathbb{E}}_{p_{\mathbf{z}}} [l_p(\mathbf{z}) \cdot \langle \boldsymbol{\delta}, \mathbf{f}(\mathbf{z}) \rangle] + \hat{p}(X_p) \cdot \log \hat{\mathbb{E}}_{q_{\mathbf{z}}} [l_q(\mathbf{z}) \exp(t)] - \sum_{i=1}^{n_q} \mu_i [t_i - \langle \boldsymbol{\delta}, \mathbf{f}(\mathbf{z}^{(i)}) \rangle],$$

where μ_i are Lagrangian multipliers. First, we solve above minimization with respect to t_i (by setting the derivative to zero), and it can be seen that the optimum is attained when $\mu_i = \frac{l_q(\mathbf{z}_q^{(i)}) \exp(t_i)}{\hat{\mathbb{E}}_{q_{\mathbf{z}}} [l_q(\mathbf{z}) \exp(t)]}$, $\sum_{i=1}^{n_q} \mu_i = \hat{p}(X_p)$, $\mu_i \geq 0$. Substituting above optimality condition to the objective function, we obtain

$$\max_{\mu_i \geq 0, \sum_{i=1}^{n_q} \mu_i = \hat{p}(X_p)} \min_{\boldsymbol{\delta}} - \hat{\mathbb{E}}_{p_{\mathbf{z}}} [l_p(\mathbf{z}) \cdot \langle \boldsymbol{\delta}, \mathbf{f}(\mathbf{z}) \rangle] + \sum_{i=1}^{n_q} -\mu_i \log(\mu_i) + \mu_i \log \hat{p}(X_p) + \mu_i \log l_q(\mathbf{z}_q^{(i)}) + \mu_i \langle \boldsymbol{\delta}, \mathbf{f}(\mathbf{z}_q^{(i)}) \rangle,$$

Second, we solve the minimization with respect to $\boldsymbol{\delta}$, one can derive the optimality condition $\hat{\mathbb{E}}_{p_{\mathbf{z}}} [l_p(\mathbf{z}) \cdot \mathbf{f}(\mathbf{z})] = \sum_{i=1}^{n_q} \mu_i \mathbf{f}(\mathbf{z}_q^{(i)})$. Substituting the above optimality condition, we obtain the objective function

$$\begin{aligned} & \max_{\mu_i \geq 0, \sum_{i=1}^{n_q} \mu_i = \hat{p}(X_p)} \sum_{i=1}^{n_q} -\mu_i \log(\mu_i) + \mu_i \log l_q(\mathbf{z}_q^{(i)}) + C, \\ & \text{subject to: } \hat{\mathbb{E}}_{p_{\mathbf{z}}} [l_p(\mathbf{z}) \cdot \mathbf{f}(\mathbf{z})] = \sum_{i=1}^{n_q} \mu_i \mathbf{f}(\mathbf{z}_q^{(i)}) \end{aligned}$$

where $C = \hat{p}(X_p) \log \hat{p}(X_p)$. The above objective function is equivalent to (13) when $R_n = 0$.

12 Proof of Theorem 3

Similar to Theorem 1, we consider optimizing δ with a constraint $\delta \in \Delta_n$.

First, due to the optimization constraint in (13) we know:

$$\begin{aligned}
\frac{R_3}{\sqrt{n_p \wedge n_q}} &\geq R_n \geq \left\| \hat{\mathbb{E}}_{p_z} [l_p(\mathbf{z}) \mathbf{f}(\mathbf{z})] - \sum_{i=1}^{n_q} \hat{\mu}_i \mathbf{f}(\mathbf{z}^{(i)}) \right\| \\
&= \left\| \hat{\mathbb{E}}_{p_z} [l_p(\mathbf{z}) \mathbf{f}(\mathbf{z})] - \hat{p}(X_p) \hat{\mathbb{E}}_{q_z} [w_q^* \mathbf{f}(\mathbf{z})] + \hat{p}(X_p) \hat{\mathbb{E}}_{q_z} [w_q^* \mathbf{f}(\mathbf{z})] - \sum_{i=1}^{n_q} \hat{\mu}_i \mathbf{f}(\mathbf{z}^{(i)}) \right\| \\
&\geq - \left\| \hat{\mathbb{E}}_{p_z} [l_p(\mathbf{z}) \mathbf{f}(\mathbf{z})] - \hat{p}(X_p) \hat{\mathbb{E}}_{q_z} [w_q^* \mathbf{f}(\mathbf{z})] \right\| + \left\| \hat{p}(X_p) \hat{\mathbb{E}}_{q_z} [w_q^* \mathbf{f}(\mathbf{z})] - \sum_{i=1}^{n_q} \hat{\mu}_i \mathbf{f}(\mathbf{z}_q^{(i)}) \right\| \\
&= - \|\nabla_{\delta} \ell(\delta^*)\| + \left\| \hat{p}(X_p) \hat{\mathbb{E}}_{q_z} [w_q^* \mathbf{f}(\mathbf{z})] - \sum_{i=1}^{n_q} \hat{\mu}_i \mathbf{f}(\mathbf{z}_q^{(i)}) \right\|,
\end{aligned}$$

where $w_q(\mathbf{z}; \delta^*)$ is shortened as w_q^* . As $\|\nabla_{\delta} \ell(\delta^*)\| \leq \frac{R_1}{\sqrt{n_p \wedge n_q}}$ is assumed with probability at least $1 - \epsilon_{R_1}$, we can see

$$\left\| \hat{p}(X_p) \hat{\mathbb{E}}_{q_z} [w_q^* \mathbf{f}(\mathbf{z})] - \sum_{i=1}^{n_q} \hat{\mu}_i \mathbf{f}(\mathbf{z}_q^{(i)}) \right\| \leq \frac{R_1 + R_3}{\sqrt{n_p \wedge n_q}}, \text{ with probability at least } 1 - \epsilon_{R_1}. \quad (16)$$

Moreover, let $\hat{w}_q := w_q(\mathbf{z}; \hat{\delta}')$,

$$\begin{aligned}
&\left\| \hat{p}(X_p) \hat{\mathbb{E}}_{q_z} [w_q^* \mathbf{f}(\mathbf{z})] - \sum_{i=1}^{n_q} \hat{\mu}_i \mathbf{f}(\mathbf{z}_q^{(i)}) \right\| \\
&= \left\| \hat{p}(X_p) \hat{\mathbb{E}}_{q_z} [w_q^* \mathbf{f}(\mathbf{z})] - \hat{p}(X_p) \hat{\mathbb{E}}_{q_z} [\hat{w}_q \mathbf{f}(\mathbf{z})] + \hat{p}(X_p) \hat{\mathbb{E}}_{q_z} [\hat{w}_q \mathbf{f}(\mathbf{z})] - \sum_{i=1}^{n_q} \hat{\mu}_i \mathbf{f}(\mathbf{z}_q^{(i)}) \right\| \\
&\geq \left\| \hat{p}(X_p) \hat{\mathbb{E}}_{q_z} [w_q^* \mathbf{f}(\mathbf{z})] - \hat{p}(X_p) \hat{\mathbb{E}}_{q_z} [\hat{w}_q \mathbf{f}(\mathbf{z})] \right\| - \left\| \hat{p}(X_p) \hat{\mathbb{E}}_{q_z} [\hat{w}_q \mathbf{f}(\mathbf{z})] - \sum_{i=1}^{n_q} \hat{\mu}_i \mathbf{f}(\mathbf{z}_q^{(i)}) \right\| \\
&= \left\| \hat{p}(X_p) \hat{\mathbb{E}}_{q_z} [w_q^* \mathbf{f}(\mathbf{z})] - \hat{p}(X_p) \hat{\mathbb{E}}_{q_z} [\hat{w}_q \mathbf{f}(\mathbf{z})] \right\| - E_{n_q}(\hat{\delta}') \\
&= \left\| \hat{p}(X_p) \hat{\mathbb{E}}_{q_z} [w_q^* \mathbf{f}(\mathbf{z})] - \hat{\mathbb{E}}_{p_z} [l_p(\mathbf{z}) \mathbf{f}(\mathbf{z})] + \hat{\mathbb{E}}_{p_z} [l_p(\mathbf{z}) \mathbf{f}(\mathbf{z})] - \hat{p}(X_p) \hat{\mathbb{E}}_{q_z} [\hat{w}_q \mathbf{f}(\mathbf{z})] \right\| - E_{n_q}(\hat{\delta}') \\
&= \left\| \nabla_{\delta} \ell(\delta^*) - \nabla_{\delta} \ell(\hat{\delta}') \right\| - E_{n_q}(\hat{\delta}') \\
&= \left\| \nabla_{\bar{\delta}}^2 \ell(\bar{\delta}) [\delta^* - \hat{\delta}'] \right\| - E_{n_q}(\hat{\delta}') \leq R_2 \|\delta^* - \hat{\delta}'\| - E_{n_q}(\hat{\delta}') \text{ with probability at least } 1 - \epsilon_{R_2},
\end{aligned}$$

where $\bar{\delta}$ is a parameter that is in between $\hat{\delta}$ and δ^* in a coordinate fashion.

Combining the above inequality with (16) we obtain: $\|\delta^* - \hat{\delta}'\| \leq \frac{R_1 + R_3}{R_2} \frac{1}{\sqrt{n_p \wedge n_q}} + \frac{C_0}{R_2}$ with probability at least $1 - \epsilon_{R_1} - \epsilon_{R_2}$ (union bound). Since the Δ_n has a radius $\frac{R_1 + R_3}{R_2} \frac{C_r}{\sqrt{n_p \wedge n_q}} + \frac{C_0}{R_2}$ where $C_r > 1$, $\|\delta^* - \hat{\delta}'\|$ is at the interior of Δ_n . This means that even without the constraint $\delta \in \Delta_n$, $\|\delta^* - \hat{\delta}'\| \leq \frac{R_1 + R_3}{R_2} \frac{1}{\sqrt{n_p \wedge n_q}} + \frac{C_0}{R_2}$ with probability at least $1 - \epsilon_{R_1} - \epsilon_{R_2}$.